Resonance line polarization and the Hanle effect in optically thick media. II - Case of a plane-parallel atmosphere

V. Bommier, E. Landi Degl'Innocenti, S. Sahal-Bréchot

Astron. Astrophys. 244, 383–390 (1991)

ASTRONOMY AND ASTROPHYSICS

Resonance line polarization and the Hanle effect in optically thick media

II. Case of a plane-parallel atmosphere

V. Bommier[1], E. Landi Degl'Innocenti[1,2], and S. Sahal-Bréchot[1]

[1] Laboratoire Astrophysique, Atomes et Molécules, URA 0812 du C.N.R.S., Département Atomes et Molécules en Astrophysique, Observatoire de Paris, Section de Meudon, F-92195 Meudon Cedex, France
[2] Dipartimento di Astronomia e Scienza dello Spazio, Università di Firenze, Largo E. Fermi 5, I-50125 Firenze, Italy

Received May 3, accepted September 28, 1990

Abstract. This paper is devoted to the description of the method of solution and to the presentation of some results of computations of resonance polarization and the Hanle effect for a two-level atom in an optically thick plane-parallel atmosphere. The approximation of complete redistribution in frequency is assumed. The principle of the method, which is of the *integral method* type, has been presented in Landi Degl'Innocenti et al. (1990, referred as Paper I in the present paper); in the present paper, we describe the numerical methods we have used and the results of our computations. Such results are compared with results given by other methods, of the *differential method* type, in zero magnetic field and under the hypothesis of complete frequency redistribution: a good agreement is obtained. The present method of computation, which we call the "global" method, is applied to test the validity of the results given by the iterative method, restricted to the first iteration, that we have used for computing the emergent polarization of the optically thick Hydrogen Hα line from solar prominences observed at the limb (Landi Degl'Innocenti et al. 1987), and observed on the disk (Bommier et al. 1989). It is found that the iterative method gives accurate results at the first iteration for a $J=3/2\rightarrow J'=5/2$ line, which gives an approximate representation of the Hydrogen Hα line. It is found, on the contrary, that the same method would not be valid for a $J=0\rightarrow J'=1$ line, as the results after the first iteration are very different from the results after convergence, in this last case. The results of our computations are finally presented in the form of Hanle diagrams for some magnetic field and line-of-sight geometries.

Key words: lines formation – linear polarization – Hanle effect – radiation transfer – solar prominences magnetic field

1. Introduction

This paper is devoted to describe the method of solution and to present some results of computations of resonance polarization and the Hanle effect for a two-level atom (lower level J, upper level J') in an optically thick plane-parallel atmosphere. The radiation in the atmosphere is assumed to be created either by collisional excitation towards the upper level, followed by radiative de-excitation, with a rate of collisional versus radiative de-excitation defined by:

$$\varepsilon=\frac{C_{J'J}}{A}, \tag{1}$$

with, typically:

$$\varepsilon\ll 1, \tag{2}$$

or, alternatively, by assuming the presence of an isotropic incident radiation located at the bottom of the atmosphere (at large optical depth). Near the surface, the radiation becomes anisotropic, a more intense radiation coming from the deeper layers than from the neighbouring layers, which are closer to the surface; as a consequence of resonance scattering, the radiation inside the atmosphere and emerging from its surface is linearly polarized, for any direction except for the vertical; furthermore, the linear polarization is modified by the magnetic field, in the domain of sensitivity of the Hanle effect, which is given by:

$$0.1\lesssim\Gamma=\omega_L\tau\lesssim 10, \tag{3}$$

where ω_L is the Larmor frequency, which depends on the magnetic field strength:

$$\omega_L=g_J\cdot\mu_B B/\hbar, \tag{4}$$

and where τ is the upper level life-time. At these magnetic field strengths, the Zeeman sublevels, broadened by the natural width, partially overlap and interferences (or coherences) between the corresponding wave-functions are partially destroyed. This brings to a modification of the polarization of the emitted radiation depending on the Zeeman level shifts. A depolarization, or alternatively an increase of linear polarization, and a simultaneous rotation of the polarization direction, due to the magnetic field, can be observed; these are the main features of the Hanle effect.

A proper description of the wave-functions interference effect can be obtained by using the atomic density matrix formalism (Bommier & Sahal-Bréchot 1978; Bommier 1980; Landi Degl'Innocenti 1982, 1983, 1984, 1985). The populations and coherences of the atomic density matrix are computed by solving the statistical equilibrium equations, or master equation for the atomic density matrix, including the magnetic field effect, provided that the intensity, anisotropy and polarization of the

Send offprint requests to: V. Bommier

incident radiation are known. The radiative transfer equations for the Stokes parameters have been derived, through a formalism coherent with the master equation for the atomic density matrix, by Landi Degl'Innocenti (1984). These two systems of equations have to be coupled for solving, in a self-consistent manner, the problem of radiative transfer of polarized radiation in an optically thick medium. This has been done for a two-level atom, by Landi Degl'Innocenti et al. (1990; hereafter referred to as Paper I). In this paper, the uni-dimensional case of a plane-parallel atmosphere has been tackled as a particular case of a more general formulation leading to a system of coupled integral equations for the atomic density matrix elements at any point of the medium; this method for solving the coupled problem of radiative transfer and statistical equilibrium is of the *integral method* type; complete frequency redistribution of the emitted radiation is however assumed.

Other methods could have been considered, in particular methods of the differential type. In this type of methods, the unknowns are the Stokes parameters I, Q, U, V, for each radiation direction Ω, each frequency ν and each optical depth τ. The description of the scattering process in terms of atomic physics is contained in the phase matrix. The method consists in coupling the Stokes parameters $I, Q, U, V(\Omega, \nu, \tau)$ at different depths, and at different directions for the same depth. In the method we have used, the Stokes parameters I, Q, U, V are derived, for any direction Ω of the radiation, from the computation of the atomic density matrix elements $\rho^K_Q(\tau)$, which are 6 elements only for every depth point and which are the unknowns. The method we have employed, which is of the integral type, consists in coupling these density matrix elements at different depths. In the differential method, 3 discretizations of the unknowns are needed: on Ω, on ν, on τ. In our method, only one discretization of the unknowns is achieved (on τ); it must be however noticed that 6 elements are necessary to completely describe the atomic density matrix at each depth. Another discretization (on ν) appears in the kernels computation. The discretization on Ω is completely avoided in using the density-matrix formalism. To our present knowledge, it results that the needed computer power is reduced, for our method, with respect to differential methods, to reach the same precision of the results. Our computation has been achieved on the VAX 8600 of the Meudon Observatory; as an example, the computation of the Stokes parameters emitted from a semi-infinite atmosphere ($10^{-4} \leq \tau \leq 10^3$), in the presence of an arbitrary magnetic field, with a 48 points Gauss-Hermite frequency integration and a 51 points τ-grid, takes 183 s (CPU time) and requires 900 memory K-bytes.

The aim of the present paper is to describe the numerical methods that have been used for solving the system of integral equations, after a brief recall about the equations themselves (Sect. 2), and after having given the proper equations for deriving the Stokes parameters of the emergent radiation from the values of the density matrix elements along the line-of-sight (Sect. 3). We present the numerical method in the following section (Sect. 4), with particular emphasis on the frequency integration and on the optical depth discretization. The convergence of the integrations is discussed. Finally, the results of computations are presented in Sect. 5; they are firstly compared with the results obtained through different methods in the absence of a magnetic field (Sect. 5.1); in the next subsection, our "global" method is used to study the convergence of an iterative method, which has been previously proposed for computing the emergent polarization of the optically thick Hydrogen Hα line of solar prominences observed at the limb (Landi Degl'Innocenti et al. 1987), and observed on the disk (Bommier et al. 1989); the effect of the magnetic field on resonance polarization (Hanle effect) is presented in Sect. 5.3 for some particular geometries of the magnetic field and of the incline of the line-of-sight with respect to the normal to the surface of the atmosphere.

2. Recall about the system of integral equations to be solved

These equations have been obtained in Paper I under the following hypothesis:

i) Plane-parallel atmosphere with vertical axis Oz, which is also assumed to be the quantization axis for the atomic density matrix (see Fig. (5) of Paper I);

ii) Two-level atom (lower level J, upper level J'), with collisional and radiative excitation and de-excitation;

iii) it is assumed that the impact approximation is valid for collisions, i.e. that the collision time is very small compared to the mean time between two successive collisions and between photon emissions, which is of the order of the characteristic time of evolution of the excited state; under this approximation, atom-photon and atom-perturber interactions can be decoupled and are additive in the master equation;

iv) induced emission is neglected;

v) the lower level J is assumed to be unpolarized, which means that $J=0$ or $1/2$, or, alternatively, that the coherences in the lower level are destroyed by collisions;

vi) complete frequency redistribution of the emitted radiation is assumed.

Under these hypotheses, the radiative transfer equations for the Stokes parameters can be expressed analytically in terms of the density matrix elements; the resulting expressions for the Stokes parameters can be introduced in the statistical equilibrium equations, leading to a system of integral equations coupling the atomic density matrix elements at each point of the medium. For the case of a plane-parallel atmosphere the results are given by Eq. (58) of Paper I, with the explicit expression for the kernels $K_{ij}(|\tau-\tau'|)$ given in Eq. (56) and Eq. (61) of Paper I.

3. Integration of the emitted radiation along the line-of-sight

We give hereafter some details about the line-of-sight integration that were not explicitly mentioned in Paper I.

Employing the same notations as in Paper I, the emerging Stokes parameter $S_i(\nu, \Omega)$ at a point $\boldsymbol{x}$ of the surface of the atmosphere is given by (see Eq. (15) of Paper I):

$$[S_i(\nu,\Omega)]_{\boldsymbol{x}} = \int_0^{\text{boundary}} [s_i(\nu,\Omega)]_{\boldsymbol{x}'}\, e^{-\tau_\nu(\boldsymbol{x},\boldsymbol{x}')}\, \eta_\nu(\boldsymbol{x}')\, \mathrm{d}s, \tag{5}$$

where the contribution of the isotropic source radiation at large optical depth has been neglected, and where the source function at point $\boldsymbol{x}'$ for the i^{th} Stokes parameter $[s_i(\nu,\Omega)]_{\boldsymbol{x}'}$ is given by:

$$[s_i(\nu,\Omega)]_{\boldsymbol{x}'} = \frac{A\sqrt{(2J'+1)}}{B} \sum_{KQ} w^{(K)}_{J'J}\, \rho^K_Q(\boldsymbol{x}')\, \mathcal{J}^K_Q(i,\Omega). \tag{6}$$

The absorption coefficient at frequency ν being assumed to be constant throughout the atmosphere, the optical depth between points $\boldsymbol{x}$ and $\boldsymbol{x}'$, $\tau_\nu(\boldsymbol{x},\boldsymbol{x}')$, is:

$$\tau_\nu(\boldsymbol{x},\boldsymbol{x}') = \eta_\nu |\boldsymbol{x}'-\boldsymbol{x}|, \tag{7}$$

the absorption coefficient at frequency ν being related to the absorption coefficient at the center of the line by:

$$\eta_\nu = \eta_0\, \phi(\nu_0 - \nu). \tag{8}$$

The coefficients $w^{(K)}_{J'J}$, which depend on the level quantum numbers only, and $\mathcal{T}^K_Q(i, \Omega)$, which is a geometrical tensor depending on the Stokes parameter considered and on the direction of propagation of the radiation, are defined in Landi Degl'Innocenti (1984). $\rho^K_Q(x')$ is the atomic density matrix element at point x' in the irreducible tensors representation, the quantization axis being the vertical to the atmosphere Oz.

The line-of-sight angular coordinates ψ_l and θ_l are defined in Fig. 1. The origin of the Oz coordinate (the vertical to the atmosphere) being taken on the surface of the atmosphere (see Fig. 5 of Paper I), one has:

$$s = \frac{-z}{\cos\psi_l}; \tag{9}$$

taking the optical depth at the center of the line along the Oz axis, τ, as the characteristic variable of the problem, instead of the geometrical depth s, one has:

$$\mathrm{d}s = \frac{-\mathrm{d}\tau}{\eta_0 \cos\psi_l}, \tag{10}$$

and:

$$\tau_\nu(\boldsymbol{x}, \boldsymbol{x}') = \frac{\phi(\nu_0 - \nu)}{\cos\psi_l}\tau. \tag{11}$$

One then has, for the emerging Stokes parameter $S_i(\nu, \Omega)$:

$$[S_i(\nu, \Omega)]_{\boldsymbol{x}} = \frac{A\sqrt{(2J'+1)}}{B} \sum_{KQ} w^{(K)}_{J'J}\, P^K_Q(\nu)\, \mathcal{T}^K_Q(i, \Omega), \tag{12}$$

with:

$$P^K_Q(\nu) = \int_0^{\text{boundary}} \rho^K_Q(\tau) \exp\left[-\frac{\phi(\nu_0 - \nu)}{\cos\psi_l}\tau\right] \frac{\phi(\nu_0 - \nu)}{\cos\psi_l}\,\mathrm{d}\tau. \tag{13}$$

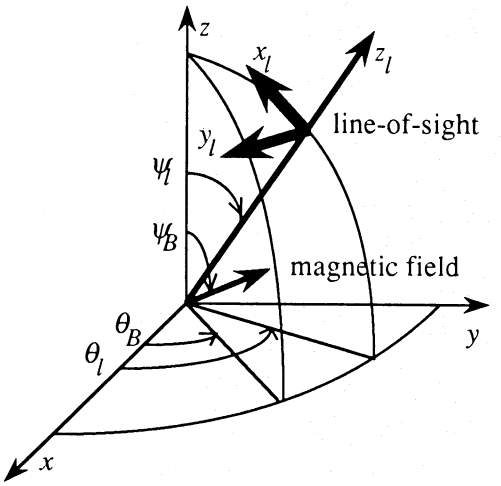

Fig. 1. Magnetic field and line-of-sight angular coordinates; the reference direction for measuring the Stokes parameters of the emitted radiation is supposed to lie in the plane containing the line-of-sight and the vertical to the atmosphere

Replacing $\mathcal{T}^K_Q(i, \Omega)$ by its value, one obtains after some computations, taking into account the conjugation property of P^K_Q:

$$[P^K_Q]^* = (-1)^{K-Q} P^K_{-Q}, \tag{14}$$

$$S_0 = \frac{A\sqrt{(2J'+1)}}{B}\left\{P^0_0 + w^{(2)}_{J'J}\left[\frac{1}{2\sqrt{2}}(3\cos^2\psi_l - 1)P^2_0 - \sqrt{3}\sin\psi_l\cos\psi_l[\cos\theta_l\,\mathrm{Re}(P^2_1) - \sin\theta_l\,\mathrm{Im}(P^2_1)] + \frac{\sqrt{3}}{2}\sin^2\psi_l[\cos 2\theta_l\,\mathrm{Re}(P^2_2) - \sin 2\theta_l\,\mathrm{Im}(P^2_2)]\right]\right\}, \tag{15}$$

$$S_1 = \frac{A\sqrt{(2J'+1)}}{B} w^{(2)}_{J'J}\left[-\frac{3}{2\sqrt{2}}\sin^2\psi_l P^2_0 - \sqrt{3}\sin\psi_l\cos\psi_l[\cos\theta_l\,\mathrm{Re}(P^2_1) - \sin\theta_l\,\mathrm{Im}(P^2_1)] - \frac{\sqrt{3}}{2}(1+\cos^2\psi_l)[\cos 2\theta_l\,\mathrm{Re}(P^2_2) - \sin 2\theta_l\,\mathrm{Im}(P^2_2)]\right], \tag{16}$$

$$S_2 = \frac{A\sqrt{(2J'+1)}}{B} w^{(2)}_{J'J}\left[\sqrt{3}\sin\psi_l[\sin\theta_l\,\mathrm{Re}(P^2_1) + \cos\theta_l\,\mathrm{Im}(P^2_1)] + \sqrt{3}\cos\psi_l[\sin 2\theta_l\,\mathrm{Re}(P^2_2) + \cos 2\theta_l\,\mathrm{Im}(P^2_2)]\right]. \tag{17}$$

4. Numerical method for solving the integral system of equations obtained in Paper I

The integral terms of the system of Eq. (58) of Paper I, coupling the atomic density matrix elements at different points of the medium, are linear combinations of integrals of the form:

$$R^{(I)}(\tau) = \int_{-\infty}^{+\infty} \mathrm{d}x\, \phi^2(x) \int_0^\infty \mathrm{d}\tau'\, E_n[|\tau - \tau'|\phi(x)]\, \rho^K_Q(\tau'), \tag{18}$$

where x is the reduced variable for frequency:

$$x = \frac{\nu - \nu_0}{\Delta\nu_D}. \tag{19}$$

Analogously, the term giving the contribution, at optical depth τ, of the external radiation supposed to illuminate the atmosphere from its bottom layer at optical depth τ_N is:

$$R^{(E)}(\tau) = \int_{-\infty}^{+\infty} \mathrm{d}x\, \phi(x) \sum_p I_p(\nu) E_{p+n}[|\tau_N - \tau|\phi(x)], \tag{20}$$

which is obtained from Eq. (51) of Paper I, supposing that the external radiation is unpolarized but eventually anisotropic (limb-darkened); the quantity $I_p(\nu)$ is defined in Eq. (50) of Paper I.

The first step is to discretize the frequency integration, the second step is to discretize the optical depth integration.

4.1. *Frequency integration*

A Doppler profile is assumed; therefore, Eq. (18) can be discretized over frequencies by using the Gauss-Hermite method, with weights W_α and abscissae x_α, ϕ_α being the profile value at x_α. One has then for $R^{(I)}(\tau)$ and $R^{(E)}(\tau)$:

$$R^{(I)}(\tau) = \sum_\alpha W_\alpha \phi_\alpha \int_0^\infty \mathrm{d}\tau'\, E_n[|\tau - \tau'|\phi_\alpha]\, \rho^K_Q(\tau'), \tag{21}$$

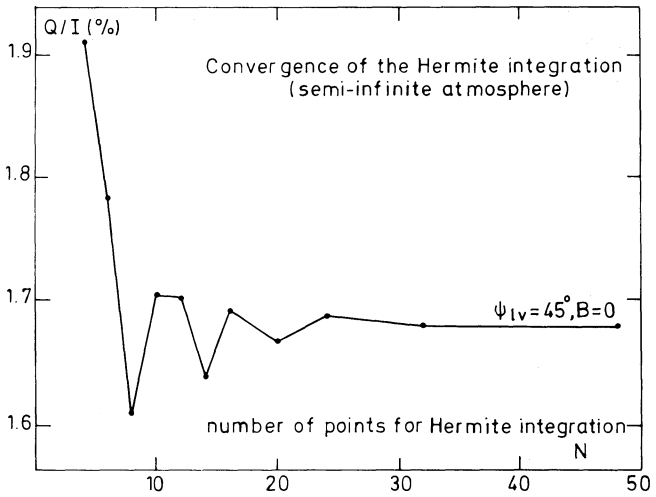

Fig. 2. Convergence of the emitted polarization at line center for $\psi_I = 45°$ (in ordinates) with respect to the number of frequency Gauss-Hermite points in the line profile (in abscissae), for a semi-infinite atmosphere ($10^{-3} \leq \tau \leq 10^4$), without collisions and magnetic field, illuminated by an isotropic radiation at large optical depths (the results of this figure are obtained with 11 depth-points for the τ integration)

$$R^{(E)}(\tau) = \sum_\alpha W_\alpha \sum_p I_{p\alpha} E_{p+n}[|\tau_N - \tau|\phi_\alpha]. \quad (22)$$

The numerical result on the convergence of the emergent polarization with respect to the number of frequency points is given in Fig. 2; it can be seen from this figure that convergence is well reached with a 32 points frequency integration.

4.2. *Optical depth discretization*

To achieve the optical depth discretization, the density matrix elements $\rho^K_Q(\tau)$ will be computed at a certain number of points $\tau_1, \ldots, \tau_N$, in logarithmic steps. $[\rho^K_Q]_i$ will denote the density matrix element at point i. We take into account the variation of $\rho^K_Q(\tau)$ between successive points $[\rho^K_Q]_i$ and $[\rho^K_Q]_{i+1}$ by introducing a linear variation of $\rho^K_Q(\tau)$:

$$\rho^K_Q(\tau) = [\rho^K_Q]_i \frac{\tau_{i+1} - \tau}{\tau_{i+1} - \tau_i} + [\rho^K_Q]_{i+1} \frac{\tau - \tau_i}{\tau_{i+1} - \tau_i} \quad \tau_i \leq \tau \leq \tau_{i+1}. \quad (23)$$

After some calculations, we obtain for the term $R^{(I)}(\tau)$ evaluated at optical depth τ_0 (τ_0 being one of the points $\tau_1, \ldots, \tau_N$):

$$R^{(I)}(\tau_0) = \sum_\alpha W_\alpha \sum_{\text{all the intervals}} \left\{ [\rho^K_Q]_a E_{n+1}[|\tau_a - \tau_0|\phi_\alpha] - [\rho^K_Q]_b E_{n+1}[|\tau_b - \tau_0|\phi_\alpha] + \frac{[\rho^K_Q]_b - [\rho^K_Q]_a}{|\tau_b - \tau_a|} \times \frac{1}{\phi_\alpha} [E_{n+2}[|\tau_a - \tau_0|\phi_\alpha] - E_{n+2}[|\tau_b - \tau_0|\phi_\alpha]] \right\}, \quad (24)$$

where a is the extreme of the interval (τ_a, τ_b) which is closest to τ_0 (and eventually coinciding with it), and b is the farthest extreme. The first line of Eq. (24) can be summed over the intervals, and one obtains:

$$R^{(I)}(\tau_0) = \sum_\alpha W_\alpha \left\{ -[\rho^K_Q]_1 E_{n+1}[|\tau_1 - \tau_0|\phi_\alpha] + 2[\rho^K_Q]_0 E_{n+1}[0] - [\rho^K_Q]_N E_{n+1}[|\tau_N - \tau_0|\phi_\alpha] + \sum_{\text{all the intervals}} \frac{[\rho^K_Q]_b - [\rho^K_Q]_a}{|\tau_b - \tau_a|} \frac{1}{\phi_\alpha} [E_{n+2} \times [|\tau_a - \tau_0|\phi_\alpha] - E_{n+2}[|\tau_b - \tau_0|\phi_\alpha]] \right\}, \quad (25)$$

$[\rho^K_Q]_0$ being $\rho^K_Q(\tau_0)$.

For the term describing the contribution of the external radiation at optical depth τ_0, one has:

$$R^{(E)}(\tau_0) = \sum_\alpha W_\alpha \sum_p I_{p\alpha} E_{p+n}[|\tau_N - \tau_0|\phi_\alpha]. \quad (26)$$

The system of integral equations is thus reduced to a system of linear equations in the unknowns $[\rho^K_Q]_i$. The number of unknowns $6 \times N$, where the factor 6 accounts for the different non-vanishing multipole components ρ^K_Q at each depth point. Once this system is solved, one can perform the τ integration contained in the definition of the quantities $P^K_Q(\nu)$ (Eq. (13)). Through the same assumption concerning the behaviour of $\rho^K_Q(\tau)$ with τ (Eq. (23)), one gets:

$$P^K_Q = [\rho^K_Q]_1 \exp\left[-\frac{\phi(\nu_0 - \nu)}{\cos\psi_I} \tau_1 \right] - [\rho^K_Q]_N \times \exp\left[-\frac{\phi(\nu_0 - \nu)}{\cos\psi_I} \tau_N \right] - \sum_{i=1}^{N-1} \left\{ \frac{\cos\psi_I}{\phi(\nu_0 - \nu)} \frac{1}{\tau_{i+1} - \tau_i} \times \left(\exp\left[-\frac{\phi(\nu_0 - \nu)}{\cos\psi_I} \tau_i \right] - \exp\left[-\frac{\phi(\nu_0 - \nu)}{\cos\psi_I} \tau_{i+1} \right] \right) \times ([\rho^K_Q]_i - [\rho^K_Q]_{i+1}) \right\}, \quad (27)$$

and, substituting this result into Eq. (15–17), the numerical values of the emerging Stokes parameters are finally recovered.

The convergence with respect to the optical depth discretization has been studied: in Fig. 3, we have plotted the emergent intensity and polarization degree in zero magnetic field, more exactly the logarithms of the differences of the values obtained assuming N and $N+10$ points in the atmosphere, as a function of $N+5$; as the slope of the curves is larger than 1, the convergence of I and Q/I is proved. In the case of Fig. 3 (semi-infinite atmosphere with $10^{-3} \leq \tau \leq 10^4$, 7 decades), it can be seen that a better than 1% relative accuracy on the emitted polarization is obtained assuming 10 points per decade; in the case of slabs of finite optical thickness, the same precision is attained assuming up to 20 points per decade. Such a rather large number of points needed to reach the convergence could be due to the discontinuities of the first derivative of $\rho^K_Q(\tau)$, which occur at the discretization points when the linear approximation of Eq. (23) is used (Frisch & Frisch 1977).

Frisch & Frisch (1977) have indeed argued that such discontinuities could lead to erroneous results of computations. We have then tried to use a better approximation, by introducing a quadratic interpolation of $\rho^K_Q(\tau)$ from its value in 3 neighbouring points $\tau_{i-1}, \tau_i, \tau_{i+1}$. But the numerical computations entering the analogous of Eq. (24) for the quadratic interpolation yield to numerical difficulties arising from the computer internal precision, so that we have been obliged to forsake this trial. However, we have compared our results, obtained through the linear approximation of Eq. (23), for the line source function at various

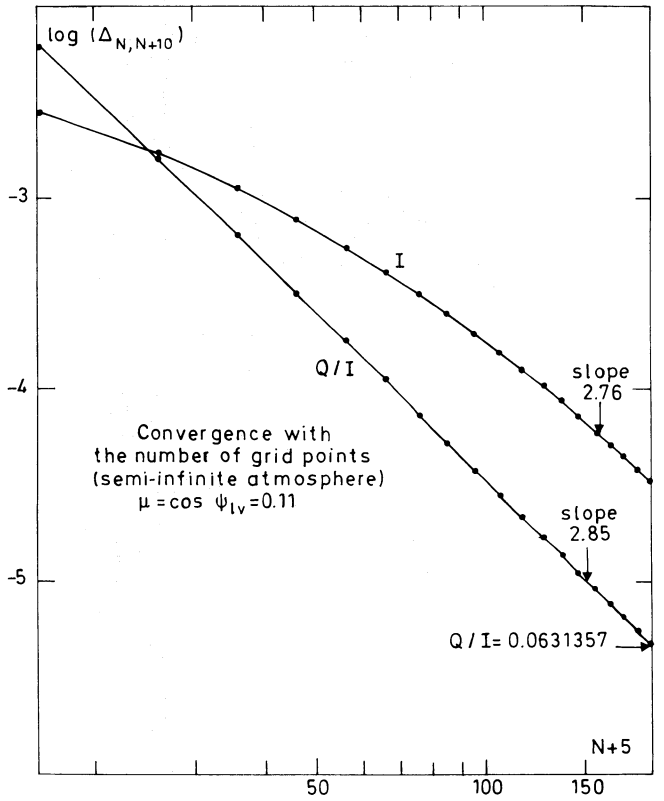

Fig. 3. Convergence of the emitted polarization at line center for $\mu=\cos\psi_l=0.11$ with respect to the number of optical depth points in a semi-infinite atmosphere ($10^{-3}\leq\tau\leq10^4$), without collisions and magnetic field, illuminated by an isotropic radiation at large optical depth: logarithms of the differences of the values of I and Q/I obtained assuming N and $N+10$ points in the atmosphere (in ordinates), as a function of $N+5$ (in abscissae); the slopes of the curves are given

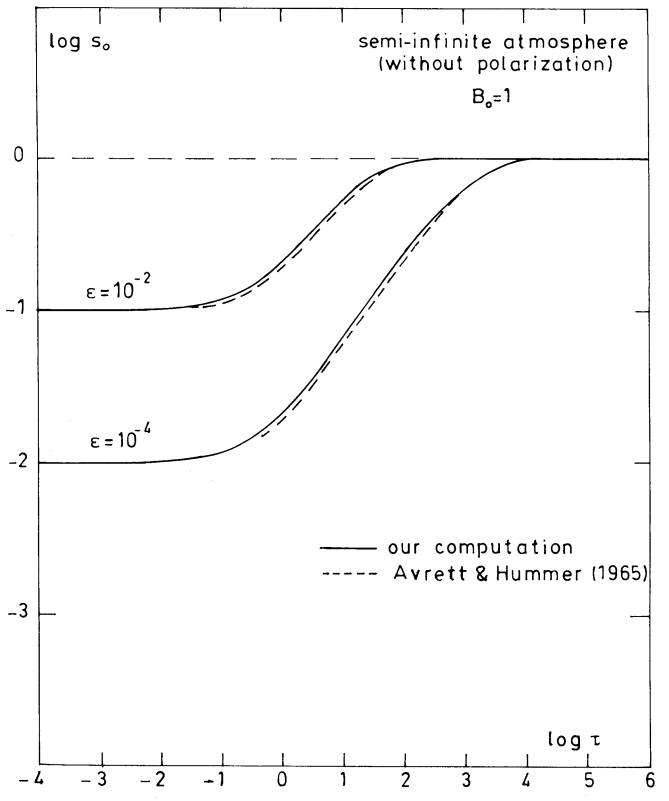

Fig. 4. Source function for the line intensity, as a function of optical depth, in logarithmic scales. The computation has been achieved neglecting the line polarization, and in zero magnetic field, for a semi-infinite atmosphere ($10^{-4}\leq\tau\leq10^6$), collisionally excited. 48 points have been assumed for the Gauss-Hermite v- integration, and enough points have been put in the τ-discretization to reach convergence

depths, in the absence of polarization and magnetic field, with those of Avrett & Hummer (1965); a satisfatory agreement has been found, as it can be seen in Fig. 4.

5. Results of computations

5.1. Comparison with results obtained with other methods in the absence of magnetic field

The emergent intensity and polarization along the line profile has been compared with results obtained by other methods, of the *differential method* type, in the absence of magnetic fields and upper the complete frequency redistribution assumption. These methods are those of Rees & Saliba (1982), and Faurobert (1987, 1988). The results are given in Fig. 5, for a semi-infinite atmosphere, and in Fig. 6 for slabs of finite optical thickness T. T is the frequency integrated optical thickness defined by:

$$T=\int_{-\infty}^{+\infty} dv\,\phi(v-v_0)\int_0^L \eta_0\,ds, \tag{28}$$

L being the slab geometrical thickness along the Oz axis. As it can be seen on these figures, a good agreement between the different methods is obtained.

5.2. Comparison global method/iterative method

The method developed in Paper I and in the present paper, which we call the "global" method, can be used to study the convergence of the iterative method, which has been used, restricted to the first iteration, for computing the emergent polarization of the optically thick Hydrogen Hα line of solar prominences observed at the limb (Landi Degl'Innocenti et al. 1987), and observed on the disk (Bommier et al. 1989).

The principle of the iterative method is the following: the contribution of the internal radiation to the statistical equilibrium equation for the atomic density matrix at optical depth τ_0 is obtained using Eq. (25), in which one introduces the density matrix elements $[\rho^K_Q]_i$ obtained at iteration $N-1$. The statistical equilibrium equations (Eq. (8) of Paper I) are then solved at each optical depth τ_i, taking eventually into account the effect of the magnetic field, which only couples the density matrix elements locally; as a result, one obtains the density matrix elements $[\rho^K_Q]_i$ at iteration N. The initial (or zero-order) solution is the solution of the coupled problem of radiative transfer and statistical equilibrium equations without polarization; in the present case, it is obtained using the global method for only the populations $[\rho^0_0]_i$, the other coherences with $K\neq0$ and $Q\neq0$ being assumed to be zero.

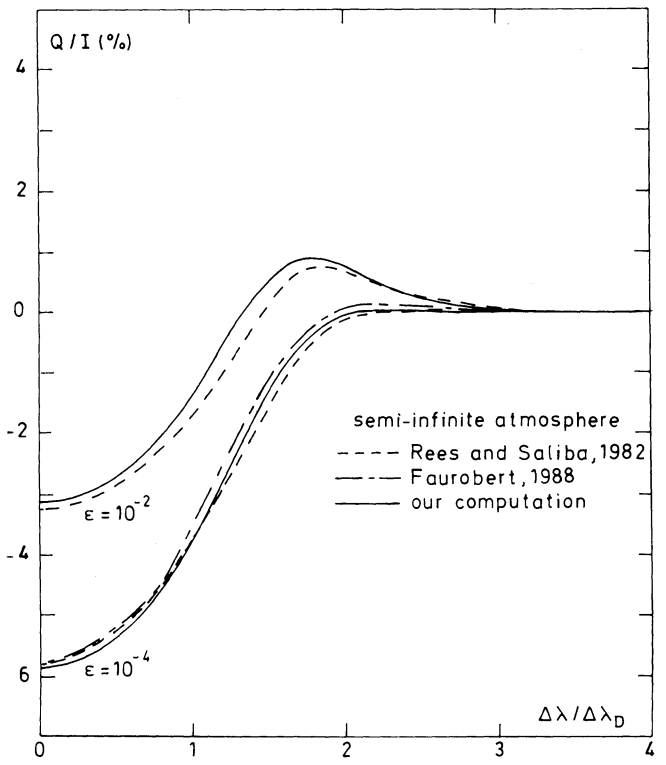

Fig. 5. Comparison of our results with those of other methods: emergent polarization for $\mu = \cos\psi_l = 0.11$ (in ordinates) as a function of reduced wavelength (in abscissae), assuming complete frequency redistribution, without magnetic field and incident radiation, for a semi-infinite atmosphere ($10^{-3} \leq \tau \leq 10^4$) with different ε values (the results of this figure are obtained with a 48 points Gauss-Hermite frequency integration, convergence being reached for the τ integration)

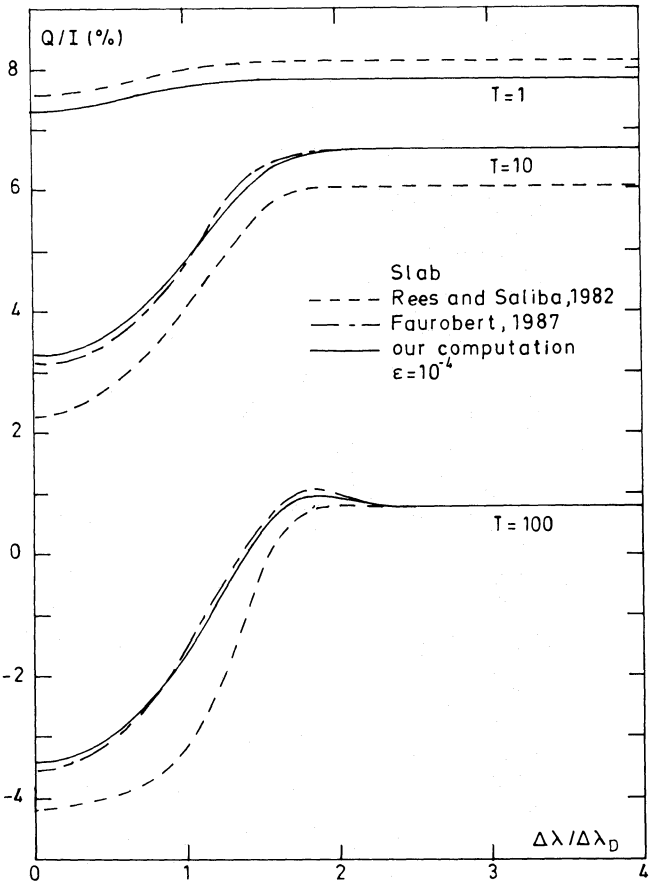

Fig. 6. Idem as Fig. 5, but for slabs of finite frequency-integrated optical thickness $T = 1, 10, 100$

The convergence of the iterative method is studied by comparing the emergent polarization obtained with the "global" method, with the one obtained with the iterative method at each iteration. This comparison has been applied to the case of a normal Zeeman triplet ($J = 0 \rightarrow J' = 1$, $w^{(2)}_{J'J} = 1$), and to the case of a $J = 3/2 \rightarrow J' = 5/2$ line ($w^{(2)}_{J'J} = 0.53$), which gives an approximate representation of the Hα line of Hydrogen. The results are shown in Fig. 7 and Fig. 8 for these two lines respectively; it can be seen from these figures that the convergence of the iterative method is reached within a few iterations, and that the convergence is more rapid for the $J = 3/2 \rightarrow J' = 5/2$ line than for the normal Zeeman triplet. This can be explained by the fact that the coupling between the density matrix elements at different points, which is proportional to $w^{(2)}_{J'J}$ and $[w^{(2)}_{J'J}]^2$, is weaker in the case of the $J = 3/2 \rightarrow J' = 5/2$ line, where $w^{(2)}_{J'J} = 0.53$, than in the case of the $J = 0 \rightarrow J' = 1$ line, where $w^{(2)}_{J'J} = 1$, which is the maximum possible value for $w^{(2)}_{J'J}$ (see Table 1 of Landi Degl'Innocenti 1984); therefore, the convergence of the iterative method is the slowest in the case of the normal Zeeman triplet, and is faster for any other line. Moreover, it can be seen from Figs. 7 and 8 that the result of the first iteration is half of the exact result, in the case of the normal Zeeman triplet, whereas for the $J = 3/2 \rightarrow J' = 5/2$ line the result of the first iteration differs from the exact result by only 0.1% in polarization. Taking into account that the present measurement uncertainties in the observation of Hα linear polarization in

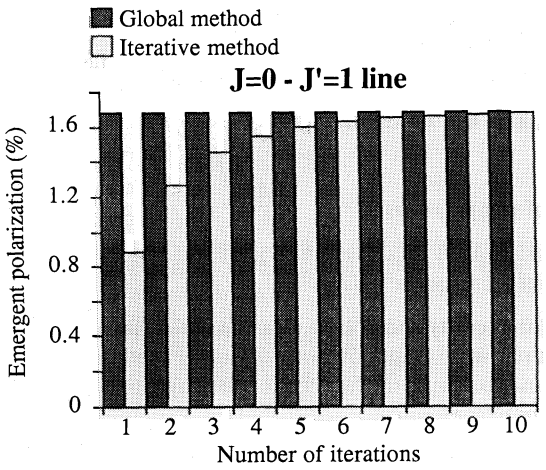

Fig. 7. Comparison of the global method with the iterative method for a normal Zeeman triplet line $J = 0 \rightarrow J' = 1$ ($w^{(2)}_{J'J} = 1$). In ordinates: Emergent polarization at line center for $\psi_l = 45°$, for a semi-infinite atmosphere ($10^{-3} \leq \tau \leq 10^4$), without collisions and magnetic field, illuminated by an isotropic radiation at large optical depth (the results of this figure are obtained with a 48 points Gauss-Hermite frequency integration and 11 depth-points for the τ integration). In abscissae: number of iterations. In dark grey: result of the global method (constant); in light grey: result of the iterative method

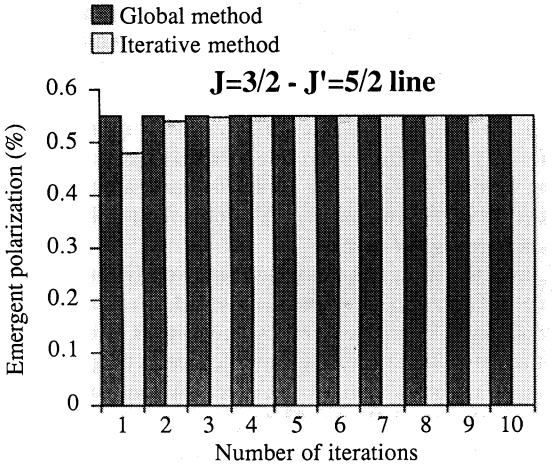

Fig. 8. Idem as Fig. 7, but for a $J=3/2 \rightarrow J'=5/2$ line ($w^{(2)}_{J'J}=0.53$), which gives an approximate representation of the Hα line of Hydrogen

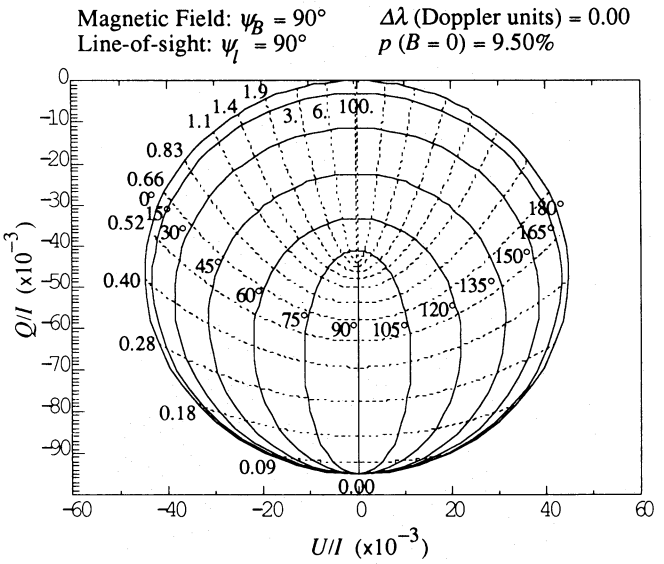

Fig. 9. Hanle effect diagram, for a semi-infinite atmosphere ($10^{-3} \leq \tau \leq 10^4$), without collisions, illuminated by an isotropic radiation at large optical depth (the results of this figure are obtained with a 48 points Gauss-Hermite frequency integration and 51 depth-points for the τ integration), for an horizontal line-of-sight ($\psi_l=90°$), and an horizontal and uniform magnetic field ($\psi_B=90°$). In full line: iso-azimuth curves (constant azimuth θ_B and increasing magnetic field strength $\Gamma=0-100$); in dotted lines: iso-strength curves (constant magnetic field strength Γ and increasing azimuth $\theta_B-\theta_l=0°-180°$). The results presented here refer to the polarization observed at line center

prominences are generally of the same order of magnitude, we conclude that the results of computations of the Hα line polarization using the iterative method restricted to the first iteration are valid for interpreting polarization measurements in terms of magnetic field diagnostic.

5.3. *Effect of a weak magnetic field (Hanle effect)*

The effect of a weak magnetic field (Hanle effect) on the linear polarization of the emitted line can be represented on diagrams, as those given in Figs. 9, 10 and 11, which have been computed

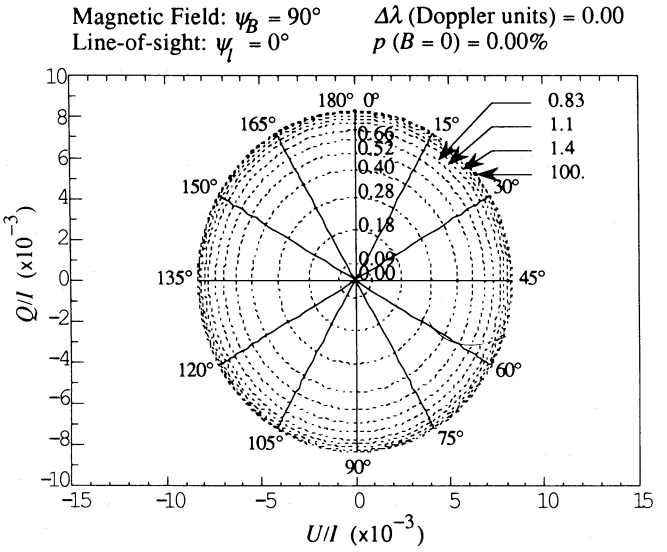

Fig. 10. Idem as Fig. 9, but for a vertical line-of-sight ($\psi_l=0°$). The magnetic field is horizontal ($\psi_B=90°$)

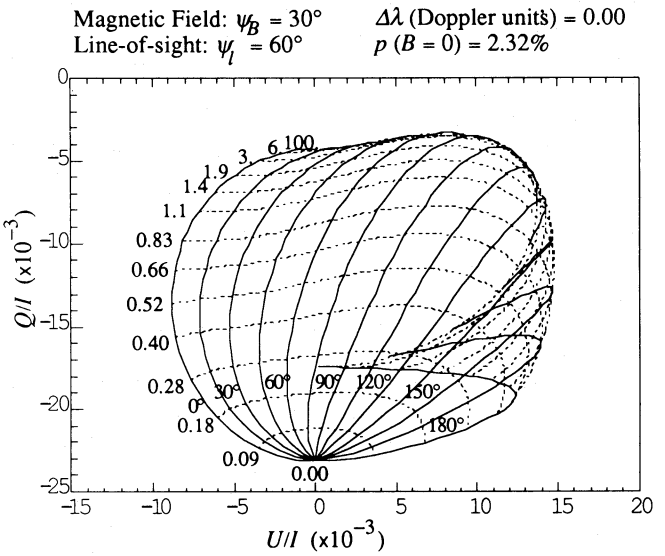

Fig. 11. Idem as Fig. 9, but for an intermediate case: $\psi_l=60°$, $\psi_B=30°$

for the following geometries:

i) a horizontal line-of-sight and a horizontal magnetic field ($\psi_l=90°$, $\psi_B=90°$);

ii) a vertical line-of-sight and an horizontal magnetic field ($\psi_l=0°$, $\psi_B=90°$);

iii) an intermediate case ($\psi_l=60°$, $\psi_B=30°$).

The full lines of the diagrams are iso-azimuth curves (constant azimuth θ_B and increasing magnetic field strength $\Gamma=0-100$), the dotted lines of the diagrams are iso-strength curves (constant magnetic field strength Γ and increasing azimuth $\theta_B-\theta_l=0°-180°$). Figure 9 shows a very close similarity with analogous diagrams obtained for an optically thin line in a 90° scattering; the usual signatures of the Hanle effect, namely a depolarization and a rotation of the polarization direction due to the magnetic field can clearly be seen on this figure; Fig. 10 shows that in this

particular scattering geometry, the effect of the magnetic field is a polarizing effect (instead of depolarizing effect as in the usual Hanle effect), the line being unpolarized in zero magnetic field ($Q=0$ and $U=0$).

In the examples given in Figs. 9, 10 and 11, the magnetic field has been assumed to be uniform in the atmosphere; however, a non-uniform magnetic field could be easily introduced in the computation, because the effect of the magnetic field is only to couple the different atomic density matrix elements at the same point in the atmosphere; in other words, the effect of the magnetic field on the density matrix is local.

6. Conclusion

In this paper, we have presented the method of solution and results of computations of resonance polarization and the Hanle effect for a two-level atom in a plane-parallel optically thick atmosphere. Our results concern not only a normal Zeeman triplet line, but any line having arbitrary quantum numbers J and J'. Complete frequency redistribution is however, assumed. The principle of the method, which is of the *integral method* type, has been presented in Landi Degl'Innocenti et al. (1990, Paper I); in the present paper, we have described the numerical methods we have used for solving our system of coupled integral equations, and we have given the results of computations. Our method of solution involves two discretizations: a frequency discretization, which has been achieved using the Gauss-Hermite method, and which is found to be convergent for 32 frequency points, and an optical depth discretization, which has been achieved assuming a linear variation of the density matrix elements between two neighbouring points; the convergence (better than 1% relative accuracy on the emitted polarization) is reached with 10 (and in some cases up to 20) points per decade; this rather large number of points necessary to reach convergence could be due to the discontinuities of the first derivative of the density matrix elements, which occur when the linear approximation is used (Frisch & Frisch 1977). Results of computations have been compared with results given by other methods, of the *differential method* type, in zero magnetic field and under the hypothesis of complete frequency redistribution: a good agreement is obtained.

The present method of computation, which we call the "global" method, has been used to study the validity of the results given by the iterative method, restricted to the first iteration, that we have previously used for computing the emergent polarization of the optically thick Hydrogen Hα line of solar prominences, for prominences observed at the limb (Landi Degl'Innocenti et al. 1987), and for prominences observed on the disk (Bommier et al. 1989). We have found that this method is valid, taking into account the uncertainties typically present in polarimetric observations, for a $J=3/2\rightarrow J'=5/2$ line which gives an approximate representation of the Hydrogen Hα line, whereas such a method would not be valid for a $J=0\rightarrow J'=1$ line, the result after the first iteration differing by approximately 50% from the results of the global method (see Figs. 7 and 8).

The results of the effect of a weak magnetic field (Hanle effect) on resonance polarization have been presented, for some magnetic field and line-of-sight geometries (see Figs. 9, 10, 11). In particular, it is shown that in some geometrical cases (Fig. 10), the effect of a magnetic field is a polarizing effect, and not a depolarizing effect as in the usual Hanle effect.

The results presented in this paper can provide a diagnostic tool for measuring weak magnetic fields in the upper solar chromosphere from the observations of linear polarization in strong resonance lines.

Acknowledgements. The numerical computations have been achieved on the VAX 8600 of the Meudon Observatory. The authors are grateful to H. Frisch, M. Faurobert and D. Rees for fruitful discussions. Part of this work has been carried out while one of the authors (E.L.D.I.) was invited as 'Professeur Associé' at the Paris-Meudon Observatory.

References

Avrett D.E., Hummer D., 1965, MNRAS 130, 295
Bommier V., Sahal-Bréchot S., 1978, A&A 69, 57
Bommier V., 1980, A&A 87, 109
Bommier V., Landi Degl'Innocenti E., Sahal-Bréchot S., 1989, A&A 211, 230
Faurobert M., 1987, A&A 178, 269
Faurobert M., 1988, A&A 194, 268
Frisch U., Frisch H., 1977, MNRAS 181, 273
Landi Degl'Innocenti E., 1982, Solar Phys. 79, 291
Landi Degl'Innocenti E., 1983, Solar Phys. 85, 3
Landi Degl'Innocenti E., 1984, Solar Phys. 91, 1
Landi Degl'Innocenti E., 1985, Solar Phys. 102, 1
Landi Degl'Innocenti E., Bommier V., Sahal-Bréchot, S., 1987, A&A 186, 335
Landi Degl'Innocenti E., Bommier V., Sahal-Bréchot S., 1990, A&A 235, 459 (Paper I)
Rees D.E., Saliba G., 1982, A&A 115, 1